Received December 2003
Reviewed April 2005
Accepted April 2005

Evaluation of subgrid scale kinetic energy models in large eddy simulations of turbulent channel flow

C.M. Winkler
The Boeing Company, St Louis, Missouri, USA, and
Sarma L. Rani
Sibley School of Mechanical and Aerospace Engineering, Cornell University, Ithaca, New York, USA

Abstract

Purpose – To evaluate the performance of different subgrid kinetic energy models across a range of Reynolds numbers while keeping the grid constant.

Design/methodology/approach – A dynamic subgrid kinetic energy model, a static coefficient kinetic energy model, and a "no-model" method are compared with direct numerical simulation (DNS) data at two friction Reynolds numbers of 180 and 590 for turbulent channel flow.

Findings – Results indicate that, at lower Reynolds numbers, the dynamic model more closely matches DNS data. As the amount of energy in the unresolved scales increases, the performance of both kinetic energy models is seen to decrease.

Originality/value – This paper provides guidance to engineers who routinely use a single grid to study a wide range of flow conditions (i.e. Reynolds numbers), and what level of accuracy can be expected by using kinetic energy models for large eddy simulations.

Keywords Eddy currents, Simulation, Channel flow

Paper type Research paper

Introduction

Large eddy simulations (LES) of turbulent channel flow is a topic of ongoing research (Gullbrand, 2004). The advantage of performing LES rather than a Reynolds averaged Navier-Stokes (RANS) simulation is that LES gives information about the instantaneous structures in the flow, as opposed to a RANS simulation which time-averages those structures into a mean flowfield. Also, LES is not restricted to low Reynolds numbers, which is a major drawback of direct numerical simulations (DNS). In LES, a low-pass filter is applied to the Navier-Stokes equations which filters out the smallest scales of motion and replaces their effect with a subgrid model. The large, energy-containing scales of motion are fully resolved in LES. Typically, the grid itself is used as the low-pass filter, giving rise to the approach known as implicit filtering, which is the most common approach in LES as no explicit filtering is applied to the governing equations.

There are many subgrid models available; a comprehensive review of available subgrid models is given in Lesieur and Metais (1996). Additionally, a more recent review may be found in Meneveau and Katz (2000). Meneveau and Katz (2000) give

International Journal of Numerical Methods for Heat & Fluid Flow
Vol. 16 No. 2, 2006
pp. 226-239

0961-5539
DOI 10.1108/09615530610644280

a detailed look at a priori and a posteriori studies along with various methods of separating the large scales from the small scales with techniques such as orthonormal basis functions. They discuss the Smagorinsky model and its limitations in detail, and they favorably review the dynamic Smagorinsky model. Bardina's similarity model is discussed, along with its mixed model variation. Testing of LES models based on comparison between real and modeled stresses is considered by reviewing the work on optimal LES approaches (Langford, 2000; Volker, 2000). Other less traditional models such as kinetic energy models and gradient models are only briefly reviewed.

Although much work has been done in LES modeling, relatively few studies have been performed which evaluate the class of kinetic energy models *a posteriori*. Kinetic energy models provide a method to directly evaluate how much energy is in the unresolved scales. To the authors' knowledge, no work has been done to evaluate how kinetic energy models perform based on the amount of energy in the unresolved scales of motion, accomplished by holding the grid fixed and increasing the Reynolds number. This will be the focus of this work. First, we will review what work has been done in the development of kinetic energy models, after which we will review what has been done in channel flow simulations.

One of the earliest works in subgrid kinetic energy models is that of Schumann (1975) who employs the use of the subgrid scale (SGS) kinetic energy, k_{sgs}, to find the eddy viscosity rather than relying on a Smagorinsky approach. He considers channels and annuli, but the key feature in this paper is his kinetic energy model. The eddy viscosity is split into two parts: the locally isotropic and inhomogeneous parts. A transport equation is developed for k_{sgs} which includes convection, production, dissipation, and diffusion. One unique approach is that the strain-rate tensor in the production term is based on the fluctuating velocities rather than the total velocities. This ensures zero production in the case of laminar flow. Some empiricism is required in order to set the constants in his model, and satisfactory agreement was obtained using the new SGS model.

Schmidt and Schumann (1989) continue the work of Schumann (1975) by investigating the convective boundary layer. No effort is made to split the SGS stresses as Schumann (1975) had originally done. Instead, a single refined transport equation for k_{sgs} is developed which includes buoyancy. To ensure non-negative values of k_{sgs}, the second-order upwind scheme is used. Also, they develop a second-order closure model for their kinetic energy equation. Fair agreement is obtained when comparing with experimental atmospheric data.

A dynamic version of the SGS kinetic energy model was proposed by Kim and Menon (1995) and compared to DNS, a dynamic eddy viscosity model, and a previous dynamic k_{sgs} model. They consider averaging their dynamic model in a local cube, but argue that this is not what a true dynamic model should entail. Instead of averaging just for the sake of numerical stability, they propose a dynamic method which requires no averaging. A method similar to the way Germano *et al.* (1991) set up the two filter system is formulated and calculations are performed for Taylor-Green vortex flow. A non-staggered grid with second-order time accuracy and fifth-order (convective terms) and sixth-order (viscous terms) spatial accuracy is used. Agreement with DNS is found to be better than the other models tested. In addition, lower computational costs are experienced when compared to the previous dynamic k_{sgs} model. By performing the simulations on two different grids, they confirm that the grid resolution was not

the deciding factor. A version of their dynamic k_{sgs} model will be described in detail in a later section of this paper.

Simulations of turbulent channel flow have been a topic of much research. Tafti and Vanka (1990) have done a detailed LES of channel flow at a Reynolds number of 180 based on channel half-height and friction velocity. Using a finite volume approach and staggered grid, they employed the Smagorinsky model to calculate the eddy viscosity. A comparison with DNS data shows good agreement, with 5 percent error in the calculated friction factor with their coarse grid ($32 \times 64 \times 32$ cells). Their fine grid ($66 \times 66 \times 66$ cells, with stretching) showed worse agreement in the means, but better agreement in turbulent statistics. They suggest that perhaps the stretching in the wall direction decreased the accuracy of the calculation and state a uniform 66×66 cross section would have worked better. Also, the use of an iterative multigrid approach in solving the pressure Poisson equations gave a significant speed up in the execution time.

Blackburn (1998) performed LES with the Smagorinsky model in conjunction with a van Driest-type wall damping function. This wall damping function essentially removes the Smagorinsky model near the wall. A friction Reynolds number of 651 is used for LES and compared with experimental results at a friction Reynolds number of 640. Satisfactory agreement in the buffer layer is obtained; however, poor agreement near the wall is attributed to experimental error. Two other simulations are conducted as well: a no-model LES on the same grid and the Smagorinsky model without a wall damping function. The no-model approach gives correct near-wall behavior, but poor results in the outer region. Without a damping function, the Smagorinsky model gives poor results in the mean flow throughout the domain. When comparing the fluctuating velocities, they find that their LES with a wall function over predicts the streamwise root mean square (rms) velocity by roughly 20 percent.

Highly resolved channel flow DNS calculations were performed by Kim *et al.* (1987) and Abe *et al.* (2001). The numerical method consists of a spectral method – Fourier series in both the spanwise and streamwise directions with Chebychev polynomials in the wall normal direction. The Reynolds number based on friction velocity and channel half-height was 180. It was found that although good agreement was obtained in the turbulence statistics, the Reynolds stresses were consistently lower than the experimental values, yet the computed vorticity near-wall fluctuations were higher than experimental results. They suggest possible error in the experiment and renormalize the experimental data by a corrected shear velocity and obtain excellent agreement except with the calculated turbulence intensities, which still remain lower than the experimentally reported values. Abe *et al.* (2001) examined the Reynolds number dependence of channel flow by performing DNS at $Re_\tau = 180$, 395, and 640. They find a greater enhancement of the spanwise and wall-normal rms velocities compared to the streamwise rms velocity as the Reynolds number is increased.

One reason that the second-order central differencing approach is popular is that it is energy conserving. However, an increase in accuracy would give less numerical dissipation and the effect of subgrid models would be more easily seen. In a recent paper by Gullbrand (2000), a conservative fourth-order code is used in turbulent channel flow. Data are compared to the results from a spectral DNS code and a second-order finite difference code. A staggered grid is used and the convective term is written in a skew-symmetric form to ensure conservation of kinetic energy.

A $128 \times 128 \times 128$ grid is used and excellent agreement is obtained at $Re_\tau = 180$ when comparing the mean and rms velocities. Little difference is shown between the second and fourth-order codes. Neither the fourth-order nor the second-order code can match the spectra produced by the spectral code at high wave numbers, which is expected due to the implicit top-hat filtering in any finite volume-type code. LES is used on a $69 \times 49 \times 48$ grid with the dynamic Smagorinsky model at $Re_\tau = 395$. The mean velocity is predicted well, while the rms quantities are underpredicted in the wall and spanwise directions, and overpredicted in the streamwise directions. Again, the spectra show that the high wave numbers are contaminated from numerical errors.

Although much work has been performed in both channel flow and kinetic energy modeling, there is a noticeable lack of information on the performance of subgrid kinetic energy models based on the amount of energy in the unresolved scales. We will examine LES of turbulent channel flow using a dynamic and static kinetic energy model, along with a no-model LES, and report on the performance of each model as the Reynolds number is varied.

Numerical procedure

The incompressible form of the three-dimensional, unsteady Navier-Stokes equations is solved using a second-order accurate finite volume method with central differencing of spatial derivatives on a non-staggered grid. The friction Reynolds number based on average friction velocity, $u_\tau = (\bar{\tau}_w/\rho_f)^{1/2}$, and channel half-height, δ, is $Re_\tau = u_\tau \delta/\nu = 180$ and 590, where $\bar{\tau}_w$, ρ_f, and ν are the mean wall shear stress, the fluid density, and the kinematic viscosity, respectively. Diffusion terms are incorporated using the Crank-Nicholson scheme and the convective terms with the second-order accurate Adams-Bashforth scheme. The Harlow-Welch fractional step method was used to decouple the continuity and momentum equations. An algebraic multigrid solver was used to solve the pressure Poisson equation resulting from the fractional step method. The equations of motion for the fluid are given by:

$$\nabla \cdot \mathbf{u} = 0 \tag{1}$$

$$\frac{\partial \mathbf{u}}{\partial t} + \nabla \cdot (\mathbf{u}\mathbf{u}) = -\nabla p + \frac{1}{Re_\tau} \nabla^2 \mathbf{u} \tag{2}$$

where the quantities have been made dimensionless by u_τ and δ. The dimensionless time scale is given by δ/u_τ. The dimensionless time step is set to 5×10^{-4}. The components of the velocity vector $\mathbf{u}$ in the streamwise, wall-normal, and spanwise directions are u, v and w, respectively. Periodic boundary conditions are applied in the spanwise and streamwise directions; zero tangential velocity and zero normal velocity are imposed at the wall.

Top-hat filtering, implemented through finite-volume implicit grid-filtering, was used to generate the equations governing the transport of the large eddies. After filtering, the equations of motion become the following:

$$\nabla \cdot \bar{\mathbf{u}} = 0 \tag{3}$$

$$\frac{\partial \bar{u}_i}{\partial t} + \frac{\partial}{\partial x_j}(\bar{u}_i \bar{u}_j) = -\frac{\partial \bar{P}}{\partial x_i} + \frac{\partial}{\partial x_j}\left[\left(\frac{1}{Re_\tau} + \nu_T\right)\frac{\partial \bar{u}_i}{\partial x_j}\right] + \frac{\partial}{\partial x_j}\left(\nu_T \frac{\partial \bar{u}_j}{\partial x_i}\right) + \delta_{i1} \quad (4)$$

The "overbar" notation denotes application of the top-hat filter. The last term on the right hand side of equation (4) represents the mean streamwise pressure gradient. The eddy viscosity, ν_T, is determined from the subgrid kinetic energy, as described in the following section.

Subgrid model formulation

Kim and Menon (1997) developed a dynamic subgrid kinetic energy model which will be summarized here for the reader. Two grids are needed for a dynamic subgrid model. The test-filter grid, having a resolution of $50 \times 50 \times 25$ in the streamwise, wall-normal, and spanwise directions, respectively, was first generated. A 2.5 percent geometric grid stretching is used in the wall normal direction on the test-filter grid. A nested grid method was used, in which each test-filter grid cell was subdivided into eight uniform fine-grid cells, which gave a final grid resolution of $100 \times 100 \times 50$. This allows for a simple and rapid process for generating a two grid system which allows easy implementation of the dynamic model when compared to agglomeration methods.

The transport equation for the subgrid kinetic energy, k_{sgs}, is given as:

$$\frac{\partial k_{\text{sgs}}}{\partial t} + \bar{u}_i \frac{\partial k_{\text{sgs}}}{\partial x_i} = \nu_T |\bar{\text{S}}|^2 - \varepsilon + \frac{\partial}{\partial x_i}\left(\nu_T \frac{\partial k_{\text{sgs}}}{\partial x_i}\right) \quad (5)$$

where the eddy viscosity, ν_T, is given by:

$$\nu_T = C_\tau \bar{\Delta} k_{\text{sgs}}^{1/2} \quad (6)$$

and the dissipation rate, ε, is given by:

$$\varepsilon = C_\varepsilon \frac{k_{\text{sgs}}^{3/2}}{\bar{\Delta}} \quad (7)$$

where $\bar{\Delta}$ is the grid scale and C_ε and C_τ are dynamically determined. The resolved strain-rate tensor, $\bar{\mathbf{S}}$, is expressed as:

$$\bar{\mathbf{S}}_{ij} = \frac{1}{2}\left(\frac{\partial \bar{u}_i}{\partial x_j} + \frac{\partial \bar{\text{u}}_j}{\partial x_i}\right) \quad (8)$$

and its magnitude is defined as:

$$|\bar{\mathbf{S}}| = \sqrt{2\bar{\text{S}}_{ij}\bar{\text{S}}_{ij}} \quad (9)$$

Let the "hat" notation symbolize the application of the test filter to a quantity and the "overbar" notation symbolize application of the grid filter. The Leonard stress tensor is then defined as:

$$\text{L}_{\text{ij}} = \widehat{\bar{u}_i \bar{u}_j} - \hat{u}_i \hat{u}_j \quad (10)$$

The kinetic energy at the test filter level can be found from the trace of (10):

$$k_{\text{test}} = \frac{1}{2}\left(\widehat{\bar{u}_k\bar{u}_k} - \hat{\bar{u}}_k\hat{\bar{u}}_k\right) \tag{11}$$

The dissipation at the test filter level is expressed as:

$$\varepsilon_{\text{test}} = (\nu + \nu_T)\left(\frac{\partial \bar{u}_i}{\partial x_j}\frac{\partial \bar{u}_i}{\partial x_j} - \frac{\partial \hat{\bar{u}}_i}{\partial x_j}\frac{\partial \hat{\bar{u}}_i}{\partial x_j}\right) \tag{12}$$

Through a similarity assumption between the subgrid stress tensor and the Leonard stress tensor, one can arrive at the following equation:

$$\mathbf{L}_{ij} = -2C_\tau\hat{\Delta}k_{\text{test}}^{1/2}\hat{\bar{\mathrm{S}}}_{ij} + \frac{1}{3}\delta_{ij}\mathbf{L}_{kk} \tag{13}$$

The least-square method of Lilly (1992) is then used to obtain a formula for C_τ:

$$C_\tau = \frac{1}{2}\frac{\mathbf{L}_{ij}\boldsymbol{\sigma}_{ij}}{\boldsymbol{\sigma}_{ij}\boldsymbol{\sigma}_{ij}} \tag{14}$$

where

$$\boldsymbol{\sigma}_{ij} = -\hat{\Delta}k_{\text{test}}^{1/2}\hat{\bar{\mathrm{S}}}_{ij} \tag{15}$$

By invoking a similarity assumption between the dissipation at the test filter and grid filter level, an equation for the dissipation at the test filter level is given as:

$$\varepsilon_{\text{test}} = C_\varepsilon\frac{k_{\text{test}}^{3/2}}{\hat{\Delta}} \tag{16}$$

One may now calculate C_τ and C_ε. These constants have been constrained to be positive in the current simulations. The advantage of the dynamic model is that no wall models need to be applied. This can be an advantage in flows where traditional wall functions may not be valid. The drawback of the dynamic model is that two grids are needed to evaluate the constants which increases the complexity of the grid generation phase of the problem.

In the model of Horiuti (1985), the constants C_τ and C_ε are held fixed rather than determined dynamically ($C_\tau = 0.05,\ \ C_\varepsilon = 1.0$). Also, to achieve correct near-wall behavior, a van Driest wall damping function was added to the Horiuti model. The damping function acted on the turbulent viscosity production and decayed in the following fashion:

$$C_\tau = 0.05\left\{1 - \exp[-(y^+/A^+)^3]\right\}^{1/2} \tag{17}$$

A^+ is a constant commonly chosen to be 26, y^+ is the nondimensional distance from the wall ($y^+ = yu_\tau/\nu$). The advantage of the Horiuti model is that only one grid needs to be generated. The drawback of the Horiuti model is that wall functions typically need to be applied which may not be known for complex flows.

Results

LES of turbulent flow in a channel of dimensions $4\pi\delta \times 2\delta \times 2\pi\delta$ in the streamwise, wall-normal and spanwise directions, respectively, were carried out for $Re_\tau = 180$ and 590, based on friction velocity u_τ and channel half-height δ. See Figure 1 for a schematic of the geometry. The results at $Re_\tau = 180$ and 590 were compared with those from the DNS of Kim *et al.* (1987) and Moser *et al.* (1999), respectively. The models studied in this work include the dynamic subgrid kinetic energy model (Kim and Menon, 1997), the static coefficient subgrid kinetic energy model (Horiuti, 1985) with a wall-damping function, and the so-called "no-model" LES, which is equivalent to a coarse grid DNS. The grid employed was $100 \times 100 \times 50$ in the streamwise, wall-normal and spanwise directions, respectively. A 2.5 percent geometric progression stretching is applied to the grid in the wall-normal direction, and a uniform grid is used in the homogeneous directions. The statistics are averaged in time and the two homogeneous (streamwise and spanwise) directions. Statistics were averaged for ten dimensionless time units (time is made dimensionless by δ/u_τ). Longer averaging times resulted in insignificant changes in the statistics. Further details and validation of the code in a turbulent square duct flow are given in Winkler *et al.* (2004).

Re_τ= 180 results

Simulations were performed at $Re_\tau = 180$ and the results compared to Kim *et al.* (1987). The mean velocity profiles are shown in Figure 2(a). Velocity and distance variables are shown in wall units ($u^+ = u/u_\tau$ and $y^+ = yu_\tau/\nu$). Results from three models are compared to the DNS data: the no-model, the Horiuti static kinetic energy model, and the dynamic kinetic energy model. In the near-wall region, all three cases compare well with the DNS data. However, near the channel centerline, all models overpredict the DNS data, with the dynamic model most closely matching the DNS data. The Horiuti model is seen to overpredict the DNS by more than ten percent, with the dynamic model overpredicting the DNS data by less than two percent.

The rms streamwise velocity (u_{rms}) profiles are shown in Figure 2(b). Here, the rms velocity is calculated as the time average of the square root of the square of the fluctuating component of velocity. It is clear that u_{rms} predicted by the dynamic model compares best with the DNS data, followed closely by the no-model case. The wall-normal rms (v_{rms}) results (Figure 2(b)) show that the no-model method compares well with the DNS data. The v_{rms} values from the kinetic energy models are

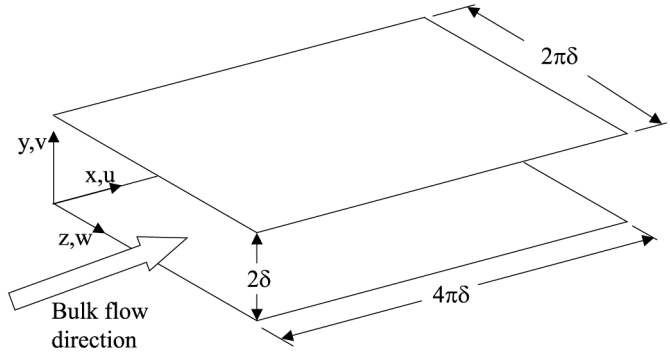

Figure 1.
Channel flow geometry for LES simulations

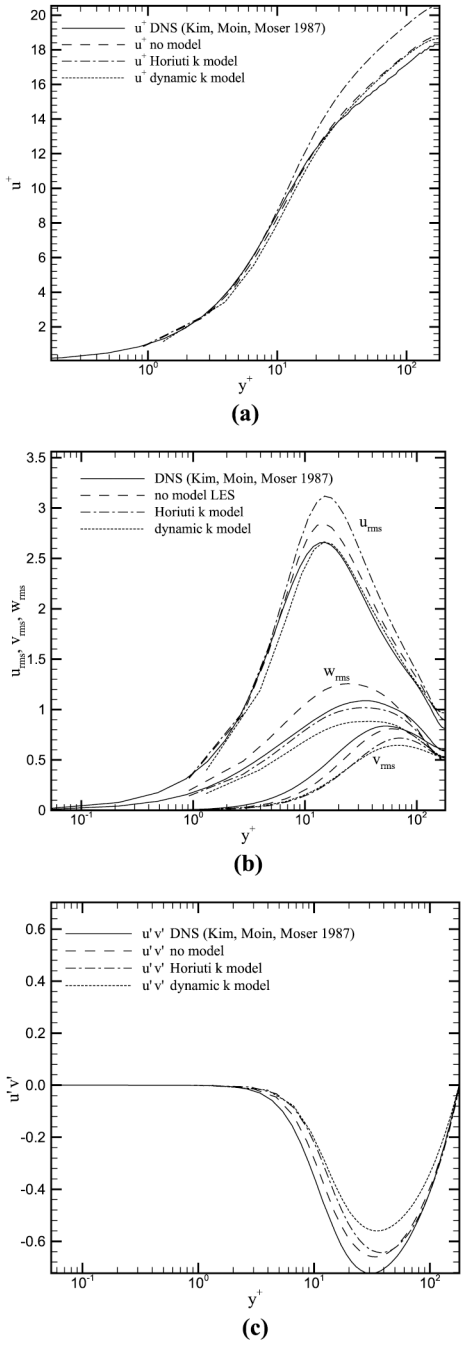

Figure 2.
(a) Mean velocity profiles, $Re_\tau = 180$; (b) RMS velocities, $Re_\tau = 180$; (c) Reynolds stress $u'v'$, $Re_\tau = 180$

underpredicted when compared to the DNS data. The spanwise rms velocity (w_{rms}) is shown in Figure 2(b). It is seen that the dynamic kinetic energy model underpredicts the DNS data by roughly 20 percent. The Horiuti model is seen to most closely match the DNS data. The no-model case overpredicts the DNS by approximately 20 percent. The Reynolds stress term, $u'v'$, is shown in Figure 2(c). It is seen that the no-model case performs best, followed closely by the Horiuti model. The dynamic model underpredicts the maximum magnitude of the term by roughly 28 percent.

The value of the SGS kinetic energy (k_{sgs}) predicted by each model is shown in Figure 3. It is clear that the dynamic model predicts roughly twice as much k_{sgs} as the Horiuti model. The non-smooth near wall behavior of k_{sgs} computed from the dynamic model can be attributed to the manner in which the fine grid is derived from the coarse grid, as two daughter cells of the coarse grid are forced to have identical production and dissipation coefficients which is a necessary numerical artifact of the model. However, the method used in the present work for implementing the dynamic model allows rapid grid generation which often is a valuable asset to industrial practice. It is seen that k_{sgs} correctly goes to zero near the wall for both models. Near the channel center, both models predict the same level of subgrid energy. The turbulent eddy viscosity, ν_T, predicted by the dynamic model is shown in Figure 4. The non-smooth nature of the dynamic model values has already been explained. It is seen that the turbulent viscosity approaches zero near the wall. The value of the coefficient for the production term, C_τ, in the dynamic model is shown in Figure 5. It is clear that the advantage of the dynamic model is that a wall model is not needed to generate correct near-wall behavior of the coefficient. The dynamic model automatically damps the production term at the wall. The Horiuti model claims this coefficient is a constant 0.05, which is roughly the mean value given by the dynamic model. The dissipation term coefficient, C_ε, in the dynamic model is shown in Figure 6. The constant coefficient models suggest a value of 1 to 1.5, which falls within the range given by the dynamic model.

Re_τ = 590 results

Here, the grid is same as the above simulations and the Reynolds number is increased to 590. In industry, typically the same grid is used for a variety of flow conditions.

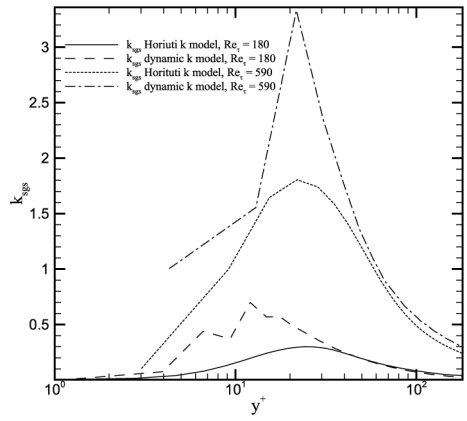

Figure 3.
Mean k_{sgs}

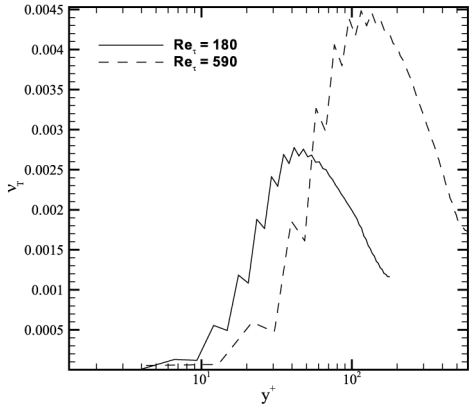

Figure 4.
Mean ν_T

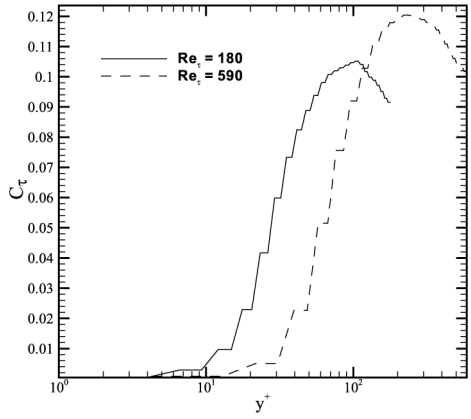

Figure 5.
Mean C_τ

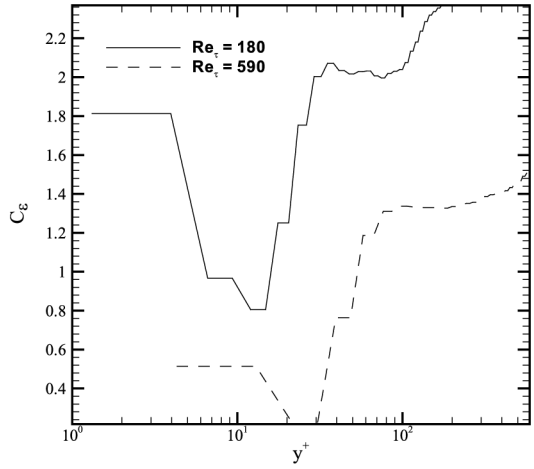

Figure 6.
Mean C_ε

By holding the grid fixed and increasing the Reynolds number, the current results will give the reader insight regarding the sensitivity of the models as a function of the amount of unresolved energy in the SGSs, as well as how various models perform relative to one another. The DNS data of Moser *et al.* (1999) are used as the baseline for comparison. The no-model approach was not used at this Reynolds number for numerical stability reasons. When examining the mean velocity profile, shown in Figure 7(a), it is clear that the qualitative trends, such as inflection points, in the DNS mean velocity profile are not captured at this Reynolds number by either k_{sgs} model. The dynamic model captures the near-wall region better than the Horituti model, yet near the centerline the dynamic model overpredicts the DNS data by roughly 20 percent.

The u_{rms} velocity profiles are shown in Figure 7(b). It is seen that neither of the two models capture the location of the peak of u_{rms} accurately. It will be shown that the amount of unresolved energy is large for this Reynolds number, and thus, the choice of a proper subgrid model is more important than at low Re_τ. The v_{rms} velocity profiles are shown in Figure 7(b). The models underpredict the DNS data as well as do not capture the location of the peak intensity. The w_{rms} velocity profiles are shown in Figure 7(b). The Horiuti model underpredicts the DNS data, while the dynamic model overpredicts the peak by roughly 19 percent. The location of the peak intensity is more closely predicted by the dynamic model. The Reynolds stress term, $u'v'$, is shown in Figure 7(c). The dynamic model predicts the DNS data the closest. The Horiuti model underpredicts the maximum magnitude of the Reynolds stress as well as gives the peak farther from the wall compared to both the DNS and the dynamic model.

The value of the subgrid kinetic energy predicted by each model is shown in Figure 3. It is clear that the dynamic model predicts roughly twice as much k_{sgs} as the Horiuti model. It is seen that k_{sgs} correctly approaches zero near the wall for both models. The turbulent eddy viscosity predicted by the dynamic model is shown in Figure 4. The non-smooth behavior of this viscosity is due to the nature of the grid used in the dynamic model formulation, as explained before. As the Reynolds number is increased, it is seen that the location of the peak of ν_T moves away from the wall as well as increases in magnitude near the channel center. The value of the coefficient for the production term in the dynamic model is shown in Figure 5. Correct near-wall behavior is seen as the production coefficient, C_τ, vanishes near the wall. Near the wall, C_τ is seen to be larger at $Re_\tau = 180$. Near the centerline, C_τ is larger at $Re_\tau = 590$. This is in agreement with the profiles of the eddy viscosity, as large production coefficients translate into large values of eddy viscosity. The coefficient for the dissipation term in the dynamic model is shown in Figure 6. The magnitude of the dissipation coefficient is seen to be smaller at all y^+ for $Re_\tau = 590$, with the minimum C_ε moving away from the wall as the Reynolds number is increased.

Conclusions

Turbulent flow in a channel was examined with LES. A dynamic and static subgrid kinetic energy model were used along with the so-called "no-model" method. Results were presented for $Re_\tau = 180$ and 590, based on friction velocity u_τ and channel half-height δ. The grid was held fixed between the two Reynolds numbers to clearly show the behavior of the subgrid models under varying levels of unresolved energy. It was seen that an advantage of the dynamic model is that no wall function is needed

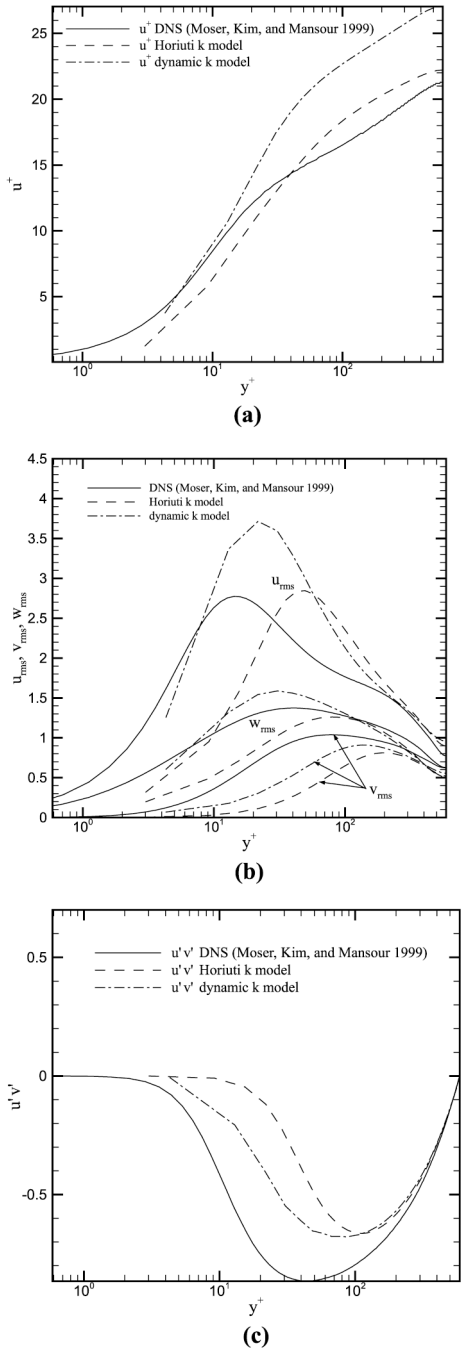

Figure 7.
(a) Mean velocity profiles, $Re_\tau = 590$; (b) RMS velocities, $Re_\tau = 590$; (c) Reynolds stress $u'v'$, $Re_\tau = 590$

to obtain correct near wall behavior of the model parameters. It was seen that results can be highly dependant on the choice of the subgrid model as well as the grid resolution, which translates directly to how much energy is contained in the unresolved scales of motion. When the amount of energy in the unresolved scales is relatively small ($Re_\tau = 180$), the dynamic model was able to closely match the DNS mean velocity profile. However, when the amount of energy in the unresolved scales is relatively large ($Re_\tau = 590$), the performance of both subgrid models is seen to decease. This is expected as all subgrid models assume a universal behavior of the small scales, and as the amount of energy in the unresolved scales is increased, this assumption breaks down due to relatively larger anisotropic scales being included as part of the unresolved scales when the grid is held fixed and the Reynolds number is increased. To the authors' knowledge, this effect has not been quantified prior to this work in this manner, which is a typical method used in industrial computational fluid mechanics practices.

Additionally, a simple method of obtaining a set of grids for use in a dynamic subgrid LES model simulation was presented. The advantage of this approach, which involves a nested grid approach, is that implementing the dynamic model is straightforward. It is seen that the nested approach gives rises to nonsmooth profiles of the dynamic model coefficients, as neighboring daughter cells are forced to have the same value of the dynamic coefficients. The single grid alternative is to use a static coefficient model, which was shown to perform nearly as well as the dynamic model when the amount of energy in the unresolved scales is large.

References

Abe, H., Kawamura, H. and Matsuo, Y. (2001), "Direct numerical simulation of a fully developed turbulent channel flow with respect to the Reynolds number dependence", *ASME J. Fluids Engineering*, Vol. 123, pp. 382-93.

Blackburn, H.M. (1998), "Channel flow LES with spectral elements", paper presented at 13th Australasian Fluid Mechanics Conference, Monash University, Melbourne.

Germano, M., Piomelli, U., Moin, P. and Cabot, W.H. (1991), "A dynamic subgrid-scale eddy viscosity model", *Phys. Fluids*, Vol. 3 No. 7, pp. 1760-5.

Gullbrand, J. (2000), "An evaluation of a conservative fourth order DNS code in turbulent channel flow", *Center for Turbulence Research Annual Research Briefs*, pp. 211-18.

Gullbrand, J. (2004), "Dynamic modeling in large-eddy simulation of turbulent channel flow: investigation of two-dimensional versus three-dimensional test filtering", *Int. J. Numerical Methods for Heat & Fluid Flow*, Vol. 14 No. 4, pp. 467-92.

Horiuti, K. (1985), "Large eddy simulation of turbulent channel flow by one-equation modeling", *Journal of the Physical Society of Japan*, Vol. 54 No. 8, pp. 2855-65.

Kim, W. and Menon, S. (1995), "A new dynamic one-equation subgrid-scale model for large eddy simulations", paper presented at 33rd Aerospace Sciences Meeting and Exhibition, Reno, NV.

Kim, W.W. and Menon, S. (1997), "Application of the localized dynamic subgrid-scale model to turbulent wall-bounded flows", *AIAA* Paper No. 97-0210.

Kim, J., Moin, P. and Moser, R. (1987), "Turbulence statistics in fully developed channel flow at low Reynolds number", *Journal of Fluid Mechanics*, Vol. 177, pp. 133-66.

Langford, J.A. (2000), "Toward ideal large eddy simulation", thesis, Dept. of Theoretical and Applied Mechanics, University of Illinois at Urbana-Champaign, Urbana, IL.

Lesieur, M. and Metais, O. (1996), "New trends in large-eddy simulations of turbulence", *Annual Review of Fluid Mechanics*, Vol. 28, pp. 45-82.

Lilly, D.K. (1992), "A proposed modification of the Germano subgrid-scale closure model", *Physics of Fluids*, Vol. 4 No. 3, pp. 633-5.

Meneveau, C. and Katz, J. (2000), "Scale-invariance and turbulence models for large-eddy simulation", *Annual Review of Fluid Mechanics*, Vol. 32, pp. 1-32.

Moser, R.D., Kim, J. and Mansour, N.N. (1999), "Direct numerical simulation of turbulent channel flow up to $Re_\tau = 590$", *Physics of Fluids*, Vol. 11, pp. 943-5.

Schmidt, H. and Schumann, U. (1989), "Coherent structure of the convective boundary layer derived from large-eddy simulation", *J. Fluid Mech.*, Vol. 200, pp. 511-62.

Schumann, U. (1975), "Subgrid scale model for finite difference simulations of turbulent flows in plane channels and annuli", *J. Computational Physics*, Vol. 18, pp. 376-404.

Tafti, D.K. and Vanka, S.P. (1990), "Large eddy simulation of channel flow using finite-difference techniques", Comp. Fluid Dynamics Laboratory Report CFD 90-01, University of Illinois at Urbana-Champaign, Urbana, IL.

Volker, S. (2000), *Optimal Large-Eddy Simulation of Turbulent Channel Flow*, Department of Mechanical Engineering, University of Illinois at Urbana-Champaign, Urbana, IL.

Winkler, C.M., Rani, S.L. and Vanka, S.P. (2004), "Preferential concentration of particles in a fully developed turbulent square duct flow", *International Journal of Multiphase Flow*, Vol. 30 No. 1, pp. 27-50.

Corresponding author
C.M. Winkler is the corresponding author and can be contacted at: chad.m.winkler@boeing.com